Canadian Technical Report of
Fisheries and Aquatic Sciences 2417

2002

NEAR FIELD CONSIDERATIONS FOR SIMRAD-MESOTECH SM 2000 MULTI-BEAM SONAR

by

N. A. Cochrane

Ocean Sciences Division
Bedford Institute of Oceanography
Department of Fisheries and Oceans
P.O. Box 1006
Dartmouth, NS
B2Y 4A2

Cat. No. Fs 97-6/2417E ISSN 0706-6457

Correct citation for this publication:

Cochrane, N. A. 2002. Near Field Considerations for Simrad-Mesotech SM 2000 Multi-beam Sonar. Can. Tech. Rep. Fish. Aquat. Sci. 2417: iv + 26p.

ABSTRACT

Cochrane, N.A. 2002. Near Field Considerations for Simrad-Mesotech SM 2000 Multi-beam Sonar. Can. Tech. Rep. Fish. Aquat. Sci. 2417: iv + 26p.

Acoustic near field effects for the Simrad-Mesotech SM 2000 multi-beam sonar significantly influence transmit and receive responses at shorter operational ranges. Three proximity dependent mechanisms are identified: 1) Inter-elemental differential phase shifts 2) Inter-elemental differential spreading losses 3) Shifts in elemental viewing aspect. The relative importance of the three mechanisms is examined at 1 m range. Near field transmit and receive and combined responses are numerically evaluated for ranges between 0.5 and 20 m. Such effects are pronounced at ranges of 5 m and less. They are characterised by both systematically reduced amplitude responses, after normal corrections for range dependent attenuation, and broadening of individual transmit-receive beam patterns at shorter ranges. Near field effects might be significantly mitigated by incorporation of phase-shift "focusing" and appropriate amplitude corrections in receive.

RÉSUMÉ

Cochrane, N.A. 2002. Near Field Considerations for Simrad-Mesotech SM 2000 Multi-beam Sonar. Can. Tech. Rep. Fish. Aquat. Sci. 2417: iv + 26p.

Les effets du champ proche acoustique du sonar multi-faisceaux Simrad-Mesotech SM 2000 influent considérablement sur les réponses d'émission et de réception aux courtes distances de fonctionnement. Trois mécanismes liés à la proximité sont établis : 1) les déphasages différentiels inter-éléments, 2) les pertes différentielles par divergence inter-éléments, et 3) les décalages de l'aspect de visualisation des éléments. L'importance relative des trois mécanismes est examinée à une distance de 1 m. Les réponses d'émission et de réception et les réponses combinées en champ proche sont évaluées par procédé numérique pour les distances entre 0,5 et 20 m. Ces effets sont prononcés aux distances de 5 m et moins. Ils se caractérisent par deux réponses à amplitude systématiquement réduite, après les corrections normales tenant compte de l'atténuation selon la distance, ainsi que par l'élargissement des profils particuliers des faisceaux d'émission et de réception aux courtes distances. Il est possible qu'on puisse réduire considérablement les effets en champ proche en incorporant un dispositif de mise au point du décalage et en apportant les corrections d'amplitude appropriées en réception.

PREFACE

This document attempts to bring together both the underlying theory and a resultant set of computed near field responses for the Simrad-Mesotech SM 2000 multi-beam sonar. While the necessary software tools and disparate computational results serving specific purposes have been in existence for several years, no previous effort has been made to document these efforts systematically for the wider user community. Such an undertaking was considered of potential utility, especially, to technical personnel performing sonar calibrations at ranges where near field considerations are mandated, but also to routine users concerned about operational performance at short ranges. The phenomenon of near field beam defocusing is not exhaustively treated. As well, only one specific implementation of the SM 2000 hardware, of several commercially available, and only one representative set of beamforming parameters are considered. At the least, we call attention to the fact that required methodologies and tools exist within DFO for more specific investigations.

INTRODUCTION

An adequate description of the acoustic "near field" is a vital consideration both for the calibration of acoustic beamforming arrays within facilities of restrictive spatial dimensions and for the quantitative interpretation of beam patterns over widely varying ranges. A common and often operationally adequate assumption is that the relevant acoustic source, receiver, or for backscatter applications, target, is effectively at infinite range when observed by or when observing the given array. Infinite range implies that ray paths between the acoustic source, receiver, or target and the discrete elements of the given array are parallel. Since this can never be precisely true for any physically realizable geometry one must initially address two questions:

1) Within what range of the array are resultant "near field" effects non-negligible (i.e. the infinite range assumption becomes inadequate) for a given application.
2) Specifically, how do "near field" effects quantitatively effect the standard beamforming process (i.e. beamforming performed with infinite range assumption).

One might also address a third question:

3) How might near field effects be mitigated by modifications to the beamforming process.

For simple circular piston radiators it is readily shown that wavelets radiated at the outer periphery cannot destructively interfere with those radiated at the center at ranges $R > a^2/\lambda$ where a is the transducer radius and λ the operational acoustic wavelength (Medwin & Clay 1997). Under these conditions the radiated pressure field decreases monotonically – but not necessarily inversely – with range. A generally accepted, but somewhat arbitrarily defined, range for true far field behaviour is given by $\pi a^2/\lambda$ or $Area/\lambda$ (*ibid.*). The latter expression is a generalization to non-circular transducers of regular form. Early considerations of the circular piston, namely the interaction of finite-sized transmit and receive elements in the near field, appear in Sabin (1964). For linear arrays analogous considerations apply. Bobber (1970) quotes $R > L^2/\lambda$ where L is the array length. Near field characteristics of more complex array geometries and/or of arrays embodying complicated elemental shadings or directivities, such as the commercial Simrad-Mesotech imaging sonar - the subject of the following discourse - are most easily investigated by numerical modeling.

The SM 2000 sonar is a circular arc array imaging sonar available in both 90 and 200 kHz versions. The considered unit operates at 200 kHz and uses an assemblage of 80 independent rectangular transducer elements (21.2 x 2.54 mm) spanning 155^0 arc (between terminal element centers) of 0.1085 m radius. Beamforming is conducted in receive only. On transmit, all array elements are excited simultaneously, in-phase, resulting in a common ensonification source for all receive beams. The transmit field is longitudinally broad and, to first order, uniform over most of the active transducer sector. On receive, internal firmware achieves a real-time synthesis of 128 equi-spaced (but not equi-width) receive beams spanning a 180^0 longitudinal sector. A significant SM 2000

design feature is that the raw elemental voltages – after amplification and firmware TVG (time variable gain) correction are also made available to the user. This permits alternative user-implemented beamforming by post-processing for specialized applications. Applicable beamforming theory, calibration methodologies, and the quantitative extraction of standard acoustic measures are discussed in Cochrane et al. (submitted). An older but excellent general overview of sonar array processing and beamforming is presented by Knight et al. (1981).

The intention is to examine SM 2000 near field effects restricted to measurement sources/receivers/targets lying within the equatorial plane of the array. Off-line beamforming as outlined below is assumed. Nevertheless, the results should also be largely applicable to real-time beamforming using the SM 2000 internal firmware when configured to use the Hamming "Low Sidelobe" window function. This is further considered in the "Discussion" section.

THEORY

Consider a circular arc array sonar synthesizing a fan of narrow and longitudinally closely spaced beams centered on and symmetric about the transducer arc's equatorial plane. Let the b^{th} beam be formed in longitudinal direction θ_b. Far field transmit and receive directivity functions for the b^{th} beam are defined by the summations of individual elemental transmit and receive contributions respectively in general longitudinal direction θ normalized by the identical summation for $\theta = \theta_b$.

$$D_S(\theta_b,\theta) = \left| \sum_{n=N_3}^{N_4} D_{e\theta}(\Delta\theta_s)\, e^{ik\Delta l_s} \right| / \left|\Sigma...\theta = \theta_b\right| \tag{1}$$

$$D_R(\theta_b,\theta) = \frac{\left| \sum_{n=N_1}^{N_2} W(\theta_b,\theta_n)\, D_{e\theta}(\Delta\theta_s)\, e^{ik\Delta l_n} e^{-ik\Delta l_s} \right|}{\sum_{n=N_1}^{N_2} W(\theta_b,\theta_n)\, D_{e\theta}(\Delta\theta_n)} \Big/ \frac{\left|\Sigma...\theta = \theta_b\right|}{\Sigma} \tag{2}$$

where

$$\Delta\theta_s = \left|\theta_n - \theta\right| \tag{3}$$

N_1 and N_2 define the summation aperture of the circular array in receive in terms of element number. N_3 and N_4 define the effective aperture of the array in transmit, namely all array elements visible from infinity in direction θ.

$D_{e\theta}(\Delta\theta_s)$ is the individual element directivity function in the θ (equatorial plane direction). For the SM 2000, elemental directivities experimentally measured for discrete mounted elements (Table 1) show a much narrower pattern (about 66^0 between –3 dB points of 20 log D) than predicted from sinc function planar radiator theory, largely due to the incorporation of projecting inter-elemental baffling.

$W(\theta_b, \theta_n)$ is the summation window weighting function applied to the n^{th} element when forming the b^{th} beam. The window function utilized is of Hamming form applied over a maximum 150^0 summation arc. It has the inherent characteristic of ensuring high side-lobe rejection in receive and, as noted above, is identical to the "Low Sidelobe" window option employed in SM 2000 real-time processing. Detailed descriptions of the window function and its mode of application appear in the Appendix.

Remaining quantities in (1) & (2) are

$$\Delta l_n = \left(1 - \cos(\Delta\theta_n)\right) r \tag{4}$$

$$\Delta\theta_n = \left|\theta_n - \theta_b\right| \tag{5}$$

and

$$\Delta l_s = \left(1 - \cos(\Delta\theta_s)\right) r \tag{6}$$

where r is the radius of the circular arc array.

A transmit response in a specific θ_b direction is chosen as an amplitude reference to express the pattern in decibel form. For what follows $\theta_b = 90^0$ is the reference direction defined by the equatorial plane radial extending outward through the longitudinal center of the transducer arc. For a properly normalized receive beamformer the (theoretical) axial[1] beamformer response will be independent of beamforming direction θ_b. The choice of normalizing reference is arbitrary. The 90^0 beam axial response is chosen.

In expression (2) the exponential terms have been explicitly separated for clarity. The exponential in Δl_n represents the standard beamformer differential phase delay for the array element at θ_n while beamforming in direction θ_b. The remaining exponential term in Δl_s represents the differential phase delay in the incident pressure wave at element θ_n arriving from infinity in direction θ. Both phase differences are measured relative to the phase appropriate to the points on the circular array periphery defined by the intersection of radials from the array center at angles θ_b and θ respectively. Referring to Fig. 1, it can be seen that expression (6) follows for a source at infinity. Similarly, expression (4) follows if beamforming angle θ_b replaces θ.

Near field responses are computed by considering a point source/receiver/target moved inward from infinity to a finite range, R, as measured from the array center of curvature

[1] The "axial" beamformer response is the response in the beamforming direction i.e. the direction for which the compensating phase delays are computed. For the outer beams a slight angular displacement of the beam amplitude maximum from the nominal beamforming (axial) direction may occur. However, the difference between the "axial" amplitude and the amplitude maximum is typically a small fraction of 1 dB making the effect difficult to discern, especially when accompanied by the marked beam broadening and response asymmetry characterizing the outer beams.

(Fig. 1). The beamformer still continues to operate assuming the source to be at infinity i.e. no attempt is made to compensate or "focus" the beamformer for the altered differential propagation ranges by adjusting the beamformer phase shifts in expression (4). In bringing the source/receiver/target to finite range one assumes range dependent spherical spreading and absorption losses to/from the nearest point on the array periphery to be compensated. While range compensation is not necessary for the computation of ratiometric directivity functions it is required for transmit and receive amplitude responses at differing ranges to be directly compared. The normally applied sonar 40 log R time variable gain (TVG) achieves this in the case of reflections (combined transmit and receive responses) from isolated targets.

For a proximate source/receiver, three effects must now be considered in computing appropriate transmit and receive responses analogous to the directivity expressions above:

1) Ray paths cease to be parallel forcing modification of expression (6) for the differential elemental phase shifts. This applies in both transmit and receive. Analogous relation (4) remains unmodified since the beamformer remains focused at infinity.

2) Circular spreading loss differentials from pressure waves propagating to and from specific array elements become non-negligible - in contrast to the case of a source/receiver at infinity. On receive, these loss differentials interact in a complicated way with the sonar applied TVG which is not constituted so as to compensate for the elemental propagation path differentials. The absorption path loss differentials are far too small to be considered.

3) On receive, the angles of incidence of the source pressure wave are systematically increased for all elements to either side of θ, consequently decreasing the amplitude of relevant elemental signals. On transmitting to a near field receiver, ray path elemental emergence angles are similarly decreased.

Each effect is considered in turn:

1) Differential phase shifts:

A range dependent replacement for expression (6) is required. From Fig. 1:

$$\begin{aligned}\Delta l_s &= l-(R-r)\\ &= (r^2\sin^2\Delta\theta_s+(R-r\cos\Delta\theta_s)^2)^{1/2}-R+r\\ &= (r^2+R^2-2rR\cos\Delta\theta_s)^{1/2}-R+r\end{aligned} \qquad (7)$$

2) Spreading & TVG differentials:

For phase shift, as opposed to time shift, type beamformers, all the stacked elemental signals are sampled simultaneously and are, therefore, subjected to identical TVG corrections. However, for simultaneously sampled elemental signals, propagation path lengths do differ. If the path differences are significant compared to the source/receiver range, signal amplitudes will vary from element to element.

Assume the incident pressure wave to have unit amplitude at the point where its position radial, i.e. the θ directional radial, intersects the circular transducer arc (or its extension). The altered path geometry requires that the unit amplitude exponential source term in (2)

$$e^{-ik\Delta l_s}$$

must be replaced by the corresponding spreading amplitude corrected term:

$$\frac{R-r}{l}e^{-ik\Delta l_s}$$

A similar modification applies in transmit using expression (1).

3) Decrements in elemental incidence/emergence angles:

$D_{e\theta}(\Delta\theta_s)$, appearing in both expressions (1) and (2) must be replaced by $D_{e\theta}(\Delta\theta_s + \alpha)$ where α is the visual angular offset of a specific array element center viewed from the near field point source/receiver/target position in Fig. 1.

$$\alpha = \text{Arc}\tan\left(\frac{r\sin\Delta\theta_s}{R - r\cos\Delta\theta_s}\right) \tag{8}$$

It will be noted that α approaches zero as range, R, approaches infinity.

Additional effects not accounted for above may also arise in the near field. For instance each ceramic element has an individual near field. Taking the worst-case latitudinal dimension, the near field range computes to about 6 cm. Therefore one remains well outside individual element near fields for all ranges considered below. Another consideration is that elemental directivity functions have been empirically measured for ceramics mounted but singly excited. With simultaneously excited array elements, adjacent element radiated pressure fields may influence the perceived radiation resistance of the medium altering the electrical characteristics of the native elements and their overall electro-acoustic efficiencies. This means that the simple addition of elemental contributions, as assumed above, may not strictly describe array characteristics for either the near or far field. However, the inter-elemental baffles designed to attenuate elemental side lobes should minimize such effects with the SM 2000.

RESULTS

In operational sonar use, SM 2000 target amplitudes at a given range vary as the product of the transmit and receive directivities. Figs. 2 & 3 show the computed array transmit and receive directivity functions at 1000 m range for a point source or receiver respectively positioned in the axial beamforming direction. These responses are normalized to the relevant response in the central (90^0) beam. Note that for this result and those below, stated "range" refers to the distance of the point source/receiver/target from the center of curvature of the sonar array. Since the sonar time series initiates at transmission of the pulse from the array surface, the time series derived range will be equal to the center of curvature range diminished by the sonar arc radius of 0.1085 m. This distinction is important at ranges of 3 meters or less.

The relative importance of the three near field effects in both transmit and receive is initially examined at 1 m range. Consideration of linear arrays of similar overall dimensions suggests the phase induced effects, at least, should be large at 1 m. Examples are restricted to the case of $\theta = \theta_b$ i.e. sources/targets centered within the synthesized receive beams. For computational convenience, transmit and receive responses at 1000 m are assumed representative of the array responses at infinity. The 1000 m range responses for a given direction are utilized to normalize the corresponding transmit and receive near field responses at 1 m range in the identical direction. It is assumed that propagation losses – measured to and from the nearest point on the array periphery are compensated by normal sonar TVG. Figs. 4 & 5 show the effects of ray path phase, alone, at 1 m in transmit and receive respectively. Figure pairs 6 & 7 and 8 & 9 show the isolated transmit and receive response differentials arising from the consideration of detailed ray path spreading losses and detailed elemental aspect angles respectively. The three simultaneously combined near field effects, in transmit and in receive, appear in Figs. 10 and 11 respectively. The latter two figures represent the (theoretical) total near field transmit and receive effects which should be observed with a working sonar.

The range dependence of the combined transmit – receive response differentials is the next to be examined. Figs. 12 to 19 show the combined differentials (defined by reference to the same combined responses at 1000 m range) computed as functions of identical beamforming & target angles at ranges of 0.5, 1, 1.5, 2, 3, 5, 10, and 20 m respectively. It will be noted that the plot in Fig. 13 (combined response at 1 m) is the decibel sum of the plots in Figs.10 & 11.

So far only the near field **axial** responses of discrete synthesized beams have been examined. A further consideration is the alteration of the angular response patterns of individual fixed beams as defined by echoes from an angularly moving near field target. Since the receive beamformer is "focused" at infinity a near field target defocusing effect is anticipated. Defocusing is manifested in the angular broadening of observed of combined transmit-receive beam patterns. Computed combined transmit – receive responses for the 90^0 beam are displayed in Fig. 20 for target ranges of 0.5, 1, 1.5, 2, 3, 5, 10, and 20 m. In this example the beamforming direction is held constant at 90^0 while the target is angularly moved through the beam at the stated ranges assuming normal

propagation loss corrections from the nearest point on the array periphery[1]. All values are normalized to the single target-axial response amplitude for the 90^0 beam at 1000 m.

DISCUSSION

Examination of the contributory near field effects at 1 m range in Figs. 4 – 9 reveals that, by far, phase shift induced effects dominate the transmit and receive responses. Since differential spreading effects amount only to a small fraction of 1 dB even at 1 m range they can probably be ignored for most "fisheries accuracy" applications. The contribution from elemental aspect is larger, but still somewhat less than 1 dB - except when the beamforming direction lies outside the 155^0 active arc of the transducer. Considering that the transmit response (Fig. 2), and consequently the sonar signal-to-noise ratio, rapidly falls to unacceptable levels outside the arc, the near field response tail-off due to the elemental aspect effect near the extremes of the beamforming angular range is unlikely to effect most real-world fisheries applications. Nevertheless, the residual reduction of about 0.3 dB across the central beamforming range remains marginally significant at 1 m. Further examination of the total combined responses in Figs. 12 to 19 shows that the total near field effects on beam-axial target strength, all negative, decline to less than 1 dB at 3 m target range and to about 0.5 dB at 5 m range.

With reference to the 90^0 beam total combined transmit-receive responses of Fig. 20, significant broadening of the central beam, and therefore consequent target defocusing in sonar imaging applications, is evident at ranges of 5 m and less. Beam broadening is accompanied by a systematic reduction in beam amplitude. Beam broadening for non-central beams is not examined but the same techniques are applicable.

For the linear array discussed in the "Introduction" the near field was defined by ranges $R > \cong L^2/\lambda$. It may be somewhat misleading to apply the uniform linear array derived expression to the SM 2000 since a uniformly spaced circular array projected onto a line results in, non-equally spaced elements and variable elemental response shadings not considered in the near field analysis of a simple linear array. Nevertheless, if one defines L as the line projection of the 155^0 active arc, all of which is utilized in transmit and nearly all (150^0) in receive, R computes to 6.0 meters. This result is in general agreement with the range at which the detailed circular array analysis shows amplitude reduction and beam broadening to become negligible for many practical applications. Use of a shorter receive summation arc ($< 150^0$) in beamforming should result in broader beams reducing near field effects for a given range.

Since the chief contribution to the circular array near field effects arises from anomalous propagation path, phase rotation effects on receive, significant amelioration should be achievable by implementation of a focusing beamformer. In a focusing beamformer,

[1] An independent angular reference for the target location has been assumed. With near field beam broadening, especially, the target angle for maximum combined transmit-receive response (in contrast to the source angle for maximum isolated receive response) can deviate considerably from the "axial" or beamforming direction. This is particularly important in the rapid fall-off region of the transmit response and should be properly accounted for in multi-beam sonar calibrations utilizing standard targets.

range dependent phase differentials would be precisely compensated for axial beam targets at a given range. Amplitude corrections for the remaining near field effects would also be possible for axial targets. However, correction would be less than perfect for off-axis targets and the resultant impact on individual beam patterns is clearly an area for future investigation.

Caution should be exercised in applying these results to the SM 2000 internally processed data stream. While the summation aperture and window functions employed are similar, differences exist in implementation. The elemental directivity function is not included in Simrad's receive beamforming normalization. However, this effect is almost negligible. More importantly, it is our understanding that range-specific phase compensation appropriate to either 20 or 5 m is implemented in the current real-time SM 2000 beamforming (R. Asplin, Kongsberg Simrad-Mesotech Ltd., Port Coquitlam, B.C., personal communication). Extrapolating from the above computations, focusing at 20 m should behave little differently than focusing at infinity. Focusing at 5 m range should yield small but significant improvements in near field performance for several meters about this range but substantial near field effects might still be expected to appear at ranges of 2 m and less.

It is evident that careful correction for theoretically expected near field effects may allow calibration of beamforming array type sonars, such as the SM 2000, in practical-sized indoor tanks as opposed to the typically floating, and inherently mechanically less stable, facilities otherwise required to reach far field calibration ranges. It is important that both the axial amplitude response and beam broadening effects be accounted for.

CONCLUSIONS

Theoretical models predict significant near field effects, namely beam broadening and amplitude reductions, to occur in the SM 2000 combined transmit and receive (i.e. target) responses at ranges of 5 m and less when utilizing infinite-target-range type beamforming. The most significant effect arises from proximity-induced differential phase shifts between array elements - especially in receive. Near field effects could be partially mitigated in post-processing beamforming by the implementation of "focusing type" phase and amplitude compensations.

ACKNOWLEDGEMENTS

The author thanks Kongsberg Simrad-Mesotech, and especially Project Engineer Bob Asplin, for making technical information available on their SM 2000 sonar. Discussions and encouragement from multi-beam project co-workers Gary Melvin of DFO's St. Andrews Biological Station and Yanchao Li of the Dept. of Geodesy and Geomatics Engineering, University of New Brunswick are gratefully acknowledged. The initial copy of this manuscript was reviewed by Mark Trevorrow of the Defense Research Establishment, Atlantic (DREA) and Bob Courtney of Natural Resources Canada at the Bedford Institute of Oceanography (BIO). Both reviewers made useful comments and suggestions.

This project was supported by High Priority Funding under DFO's National Hydroacoustic Program supplemented by bridge funding from DFO's Strategic Science Fund.

REFERENCES

Bobber, R. J. 1970. Underwater Electroacoustic Measurements. Naval Research Laboratory, U.S. Govt. Printing Office, Washington, D.C. 333 pp.

Cochrane, N. A., Y. Li, and G. D. Melvin. Quantification of a multi-beam sonar for fisheries assessment applications. J. Acoust. Soc. Am. (submitted).

Knight, W. C., Pridham, R. G. , and Kay, S. M. 1981. Digital signal processing for sonar. Proc. IEEE. 69: 1451 – 1506.

Medwin, H., and Clay, C. S. 1997. Fundamentals of Acoustical Oceanography. Academic Press, Boston. 712 pp.

Sabin, G. A. 1964. Calibration of piston transducers at marginal test distances. J. Acoust. Soc. Am. 36(1): 168 – 173.

Table 1. SM 2000 equatorial plane, single element directional response , $D_{e\theta}(\Delta\theta)$, based on data supplied by Kongberg Simrad-Mesotech.

Angle $\Delta\theta^0$	20 log D
0	0
2	-0.05
5	-0.14
10	-0.34
15	-0.65
20	-0.98
25	-1.61
30	-2.44
35	-3.49
40	-4.61
45	-5.77
50	-7.11
55	-8.03
60	-9.58
70	-12.5
80	-17.3
89	-21.3
>89	$-\infty$

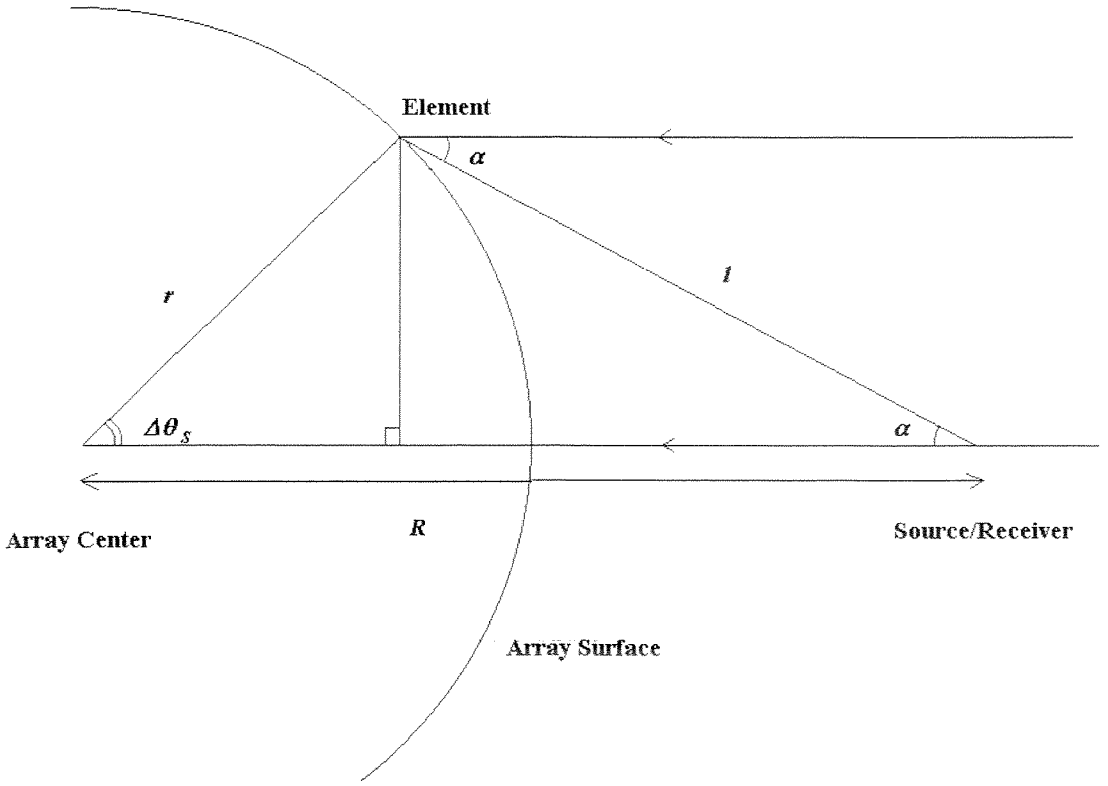

Figure 1. Fundamental beamforming geometry.

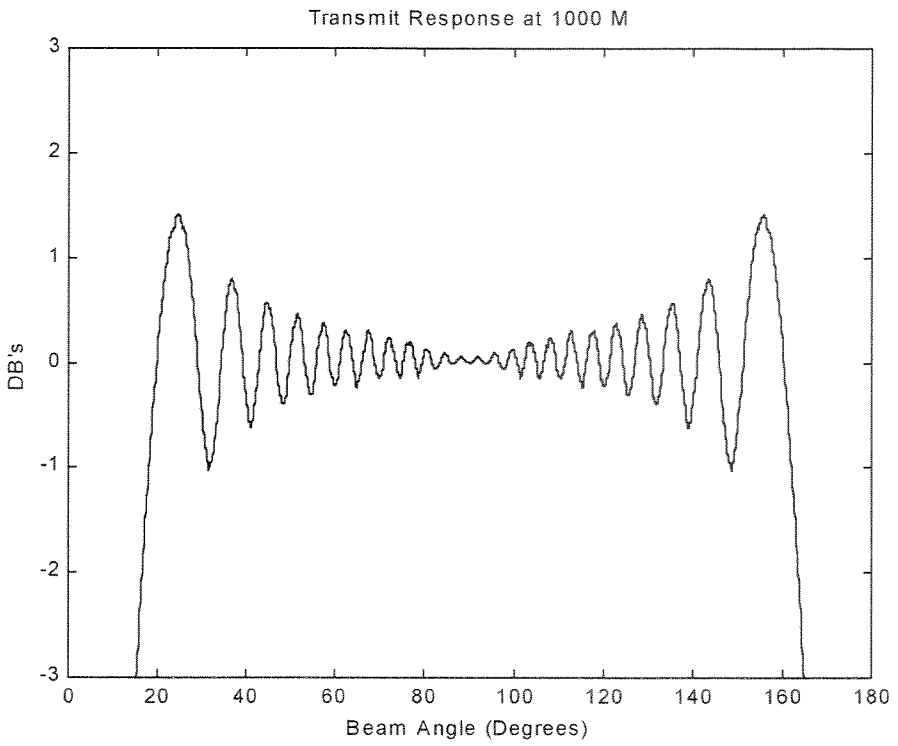

Figure 2. Transmit response at 1000 m range.

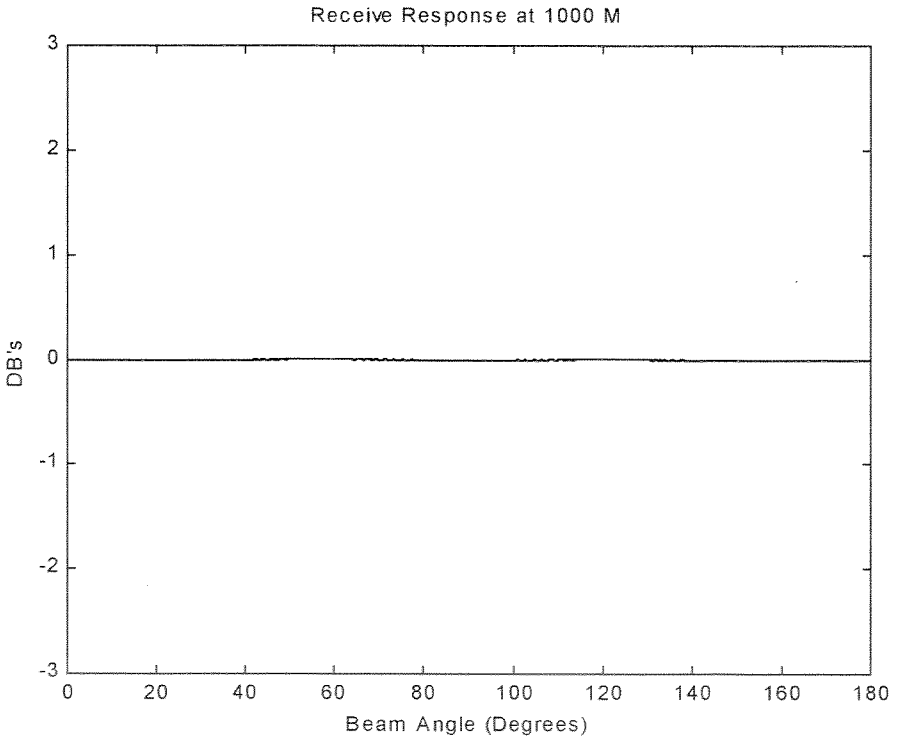

Figure 3. Receive response at 1000 m range.

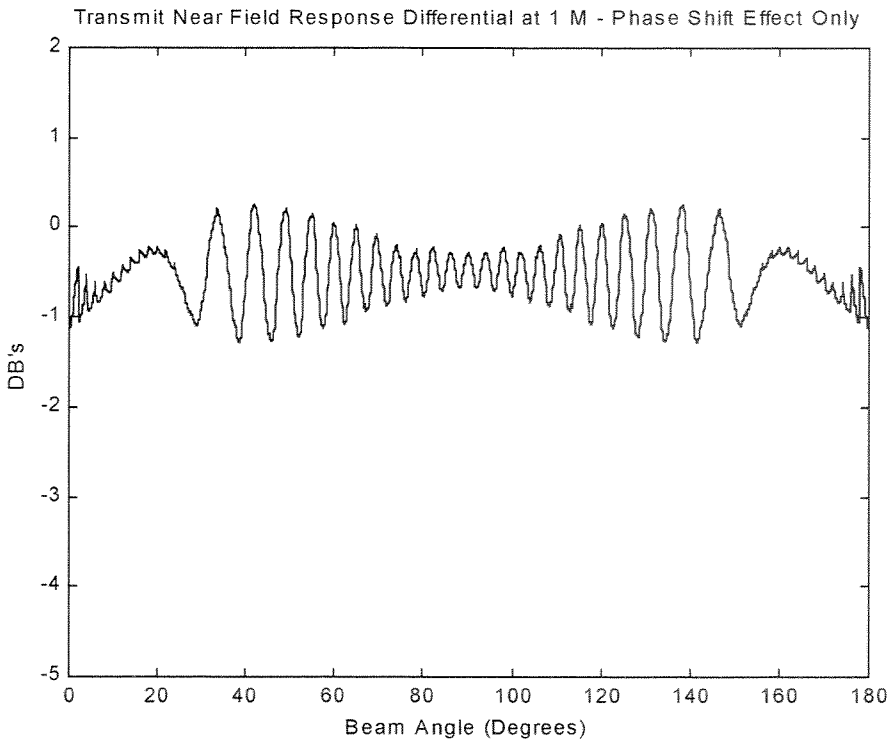

Figure 4. Effect of ray path phase in transmit at 1 m range.

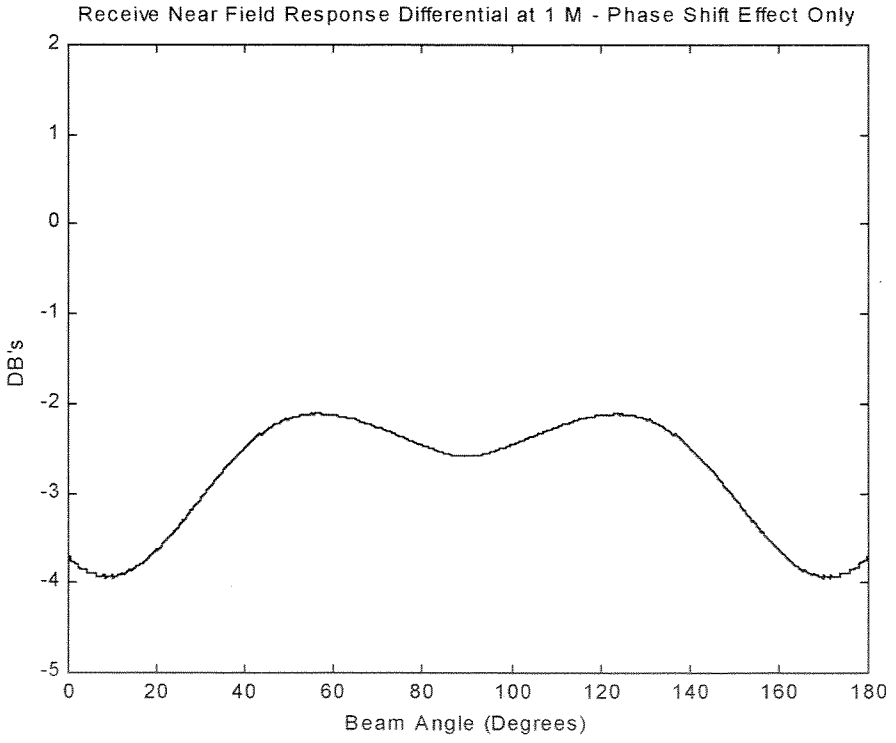

Figure 5. Effect of ray path phase in receive at 1 m range.

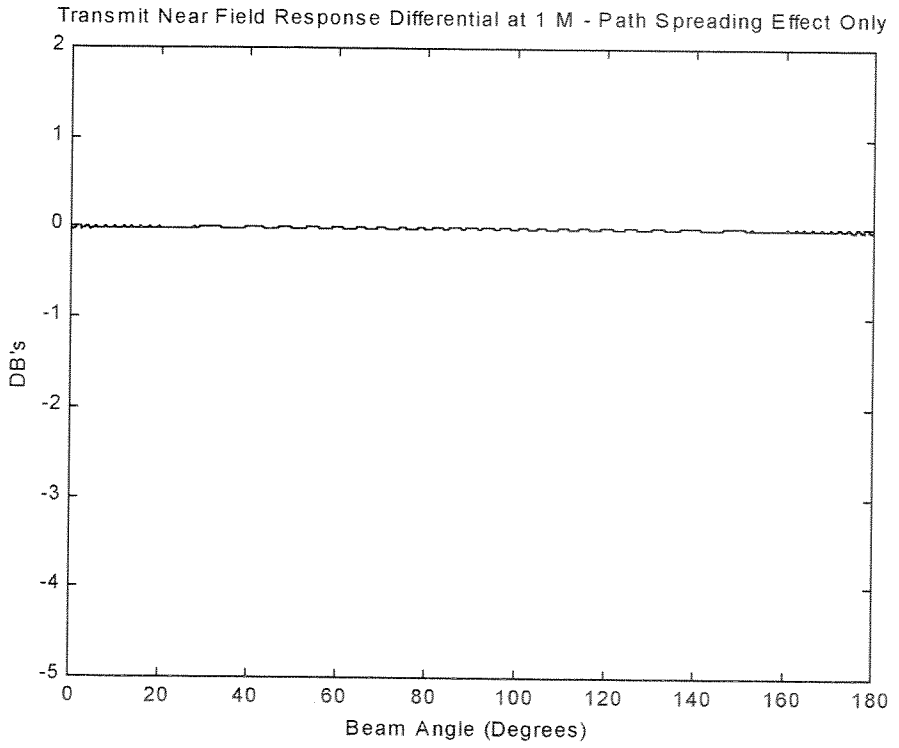

Figure 6. Effect of ray path length in transmit at 1 m range.

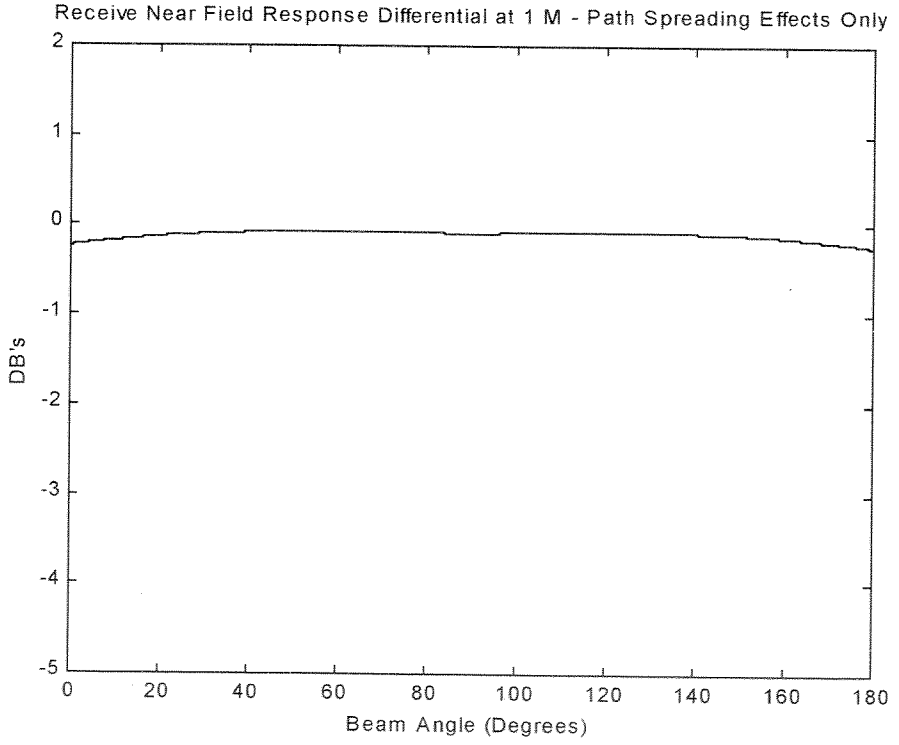

Figure 7. Effect of ray path length in receive at 1 m range.

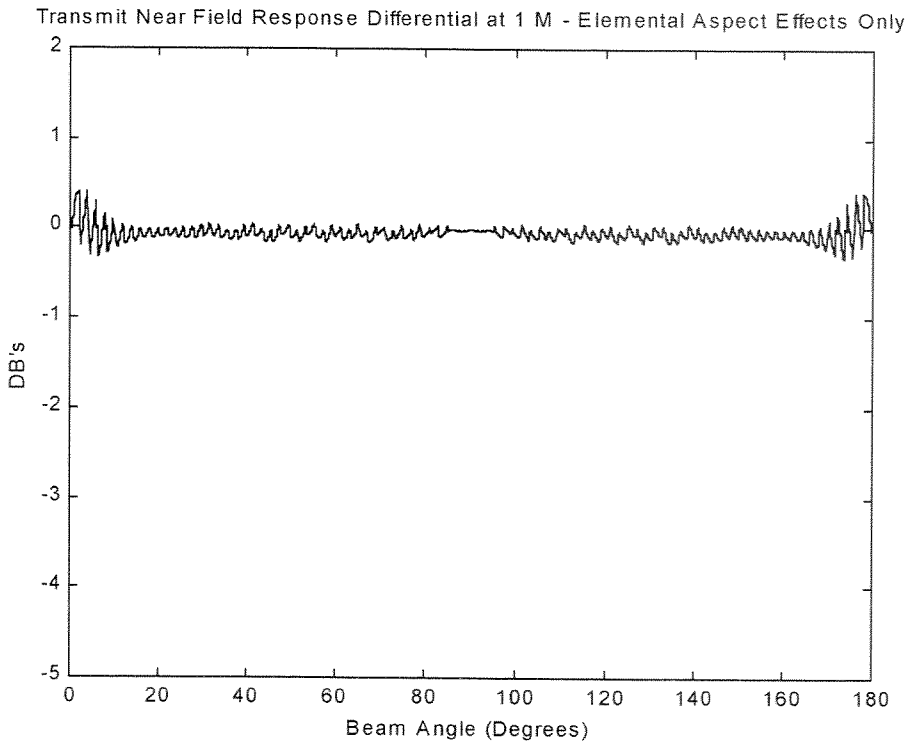

Figure 8. Effect of element aspect in transmit at 1 m range.

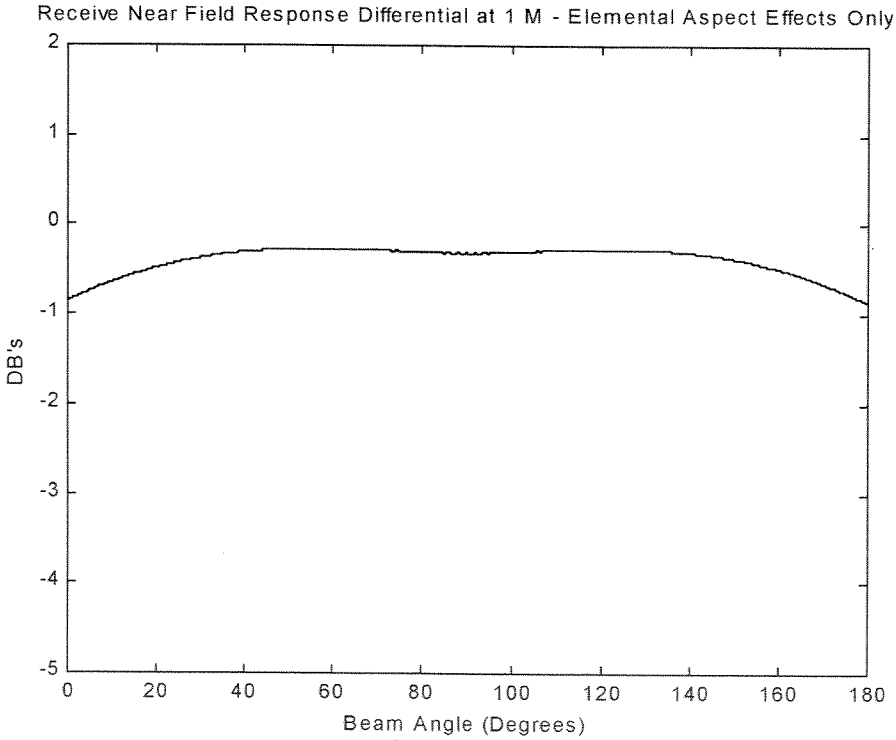

Figure 9. Effect of element aspect in receive at 1 m range.

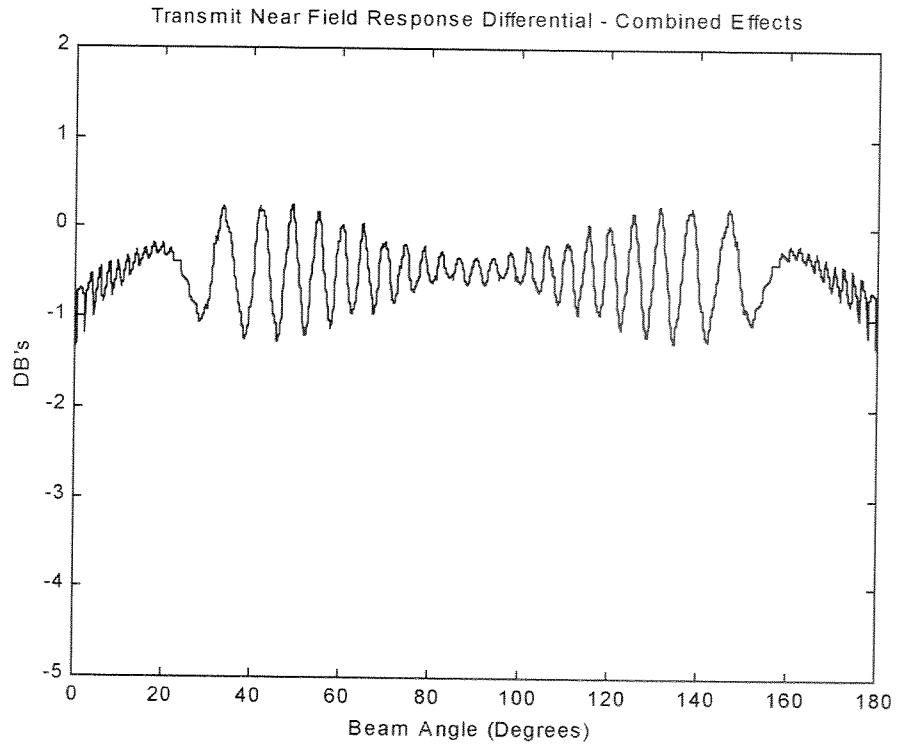

Figure 10. Combined effect transmit response at 1 m range.

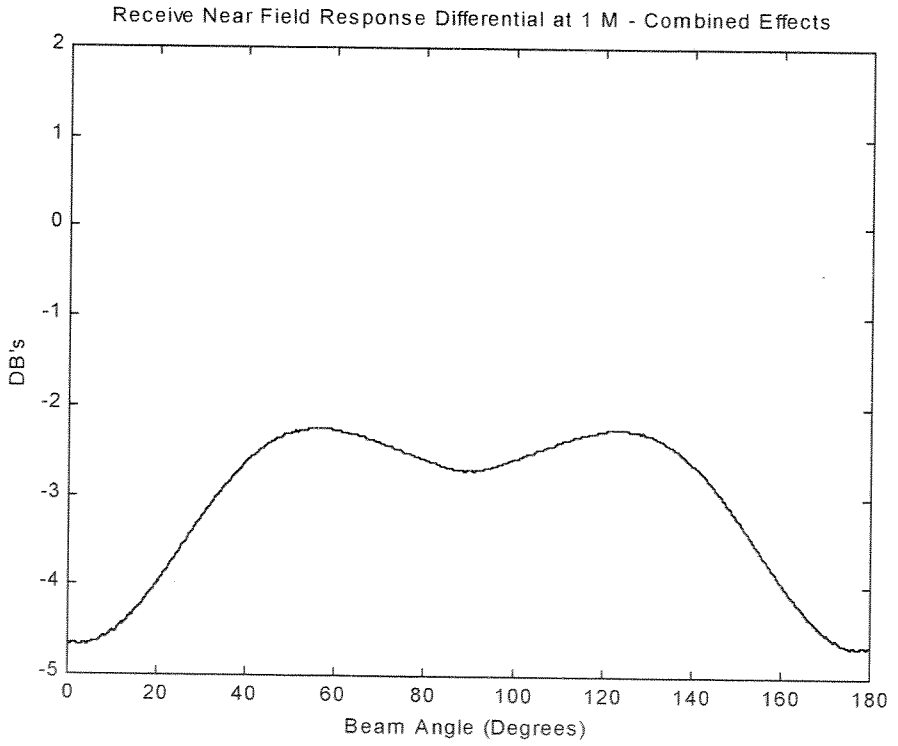

Figure 11. Combined effect receive response at 1 m range.

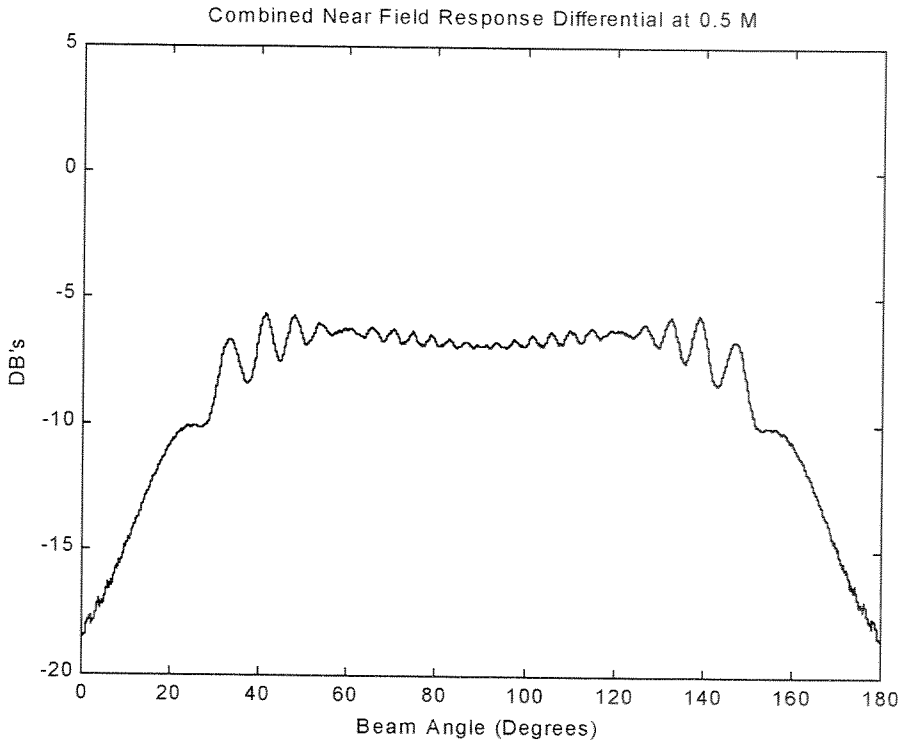

Figure 12. Combined transmit – receive near field effects at 0.5 m range.

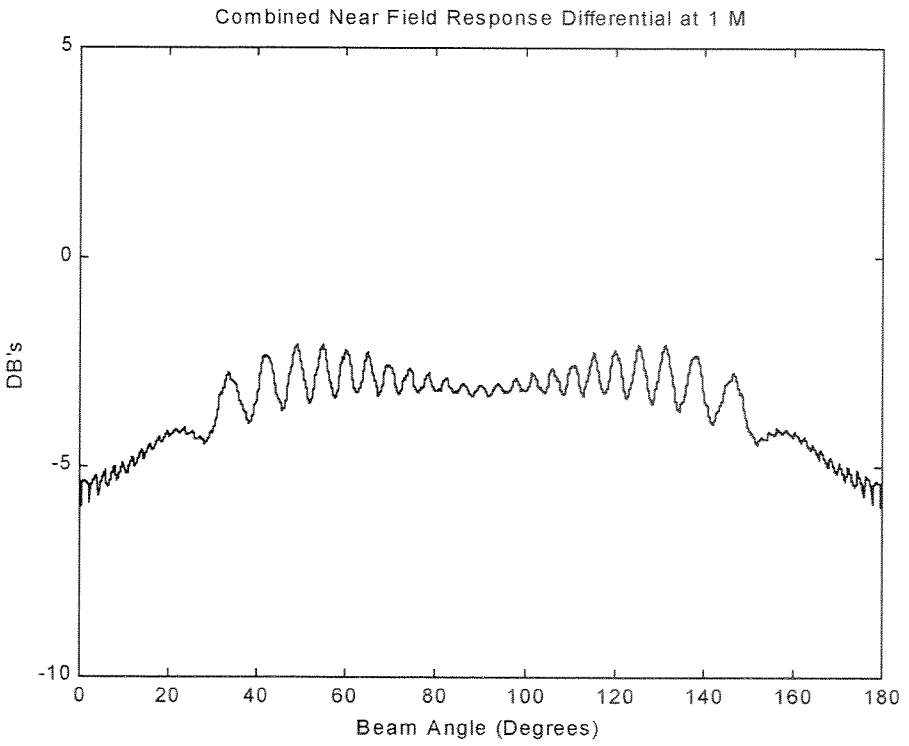

Figure 13. Combined transmit – receive near field effects at 1 m range.

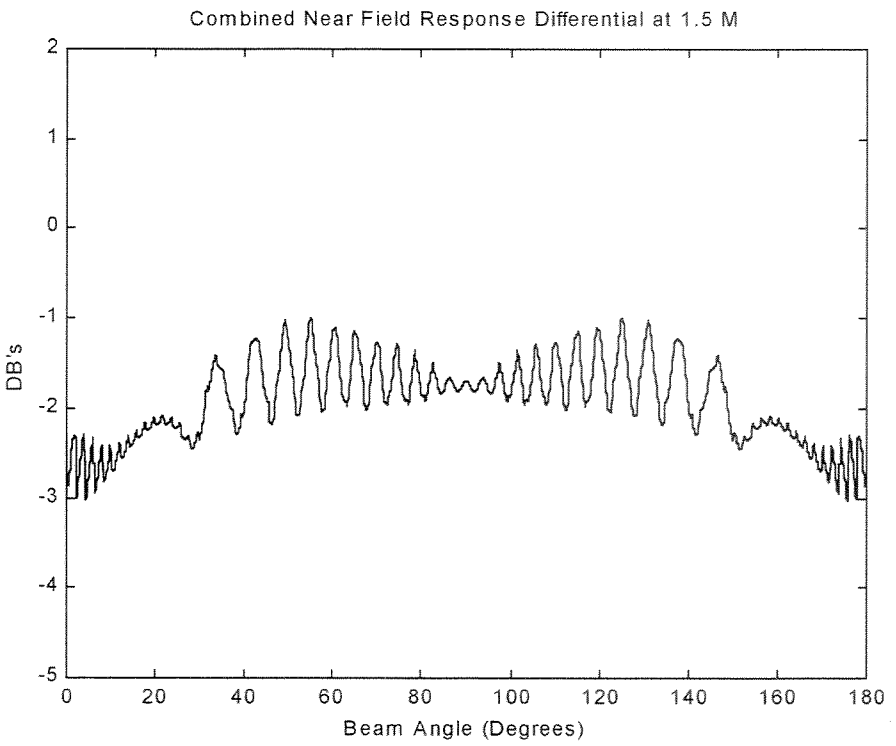

Figure 14. Combined transmit – receive near field effects at 1.5 m range.

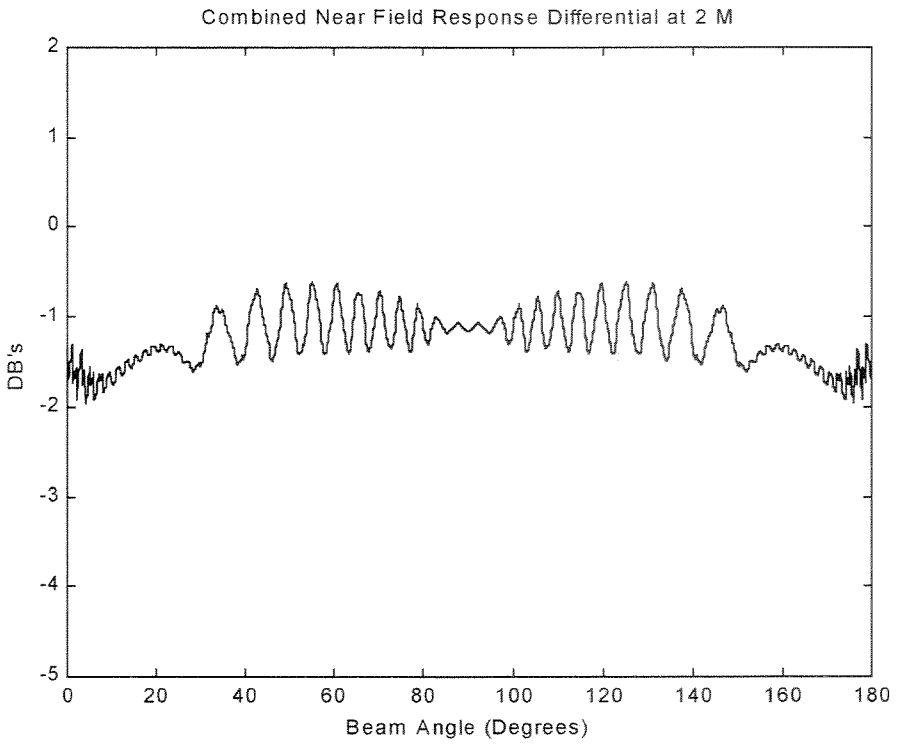

Figure 15. Combined transmit – receive near field effects at 2 m range.

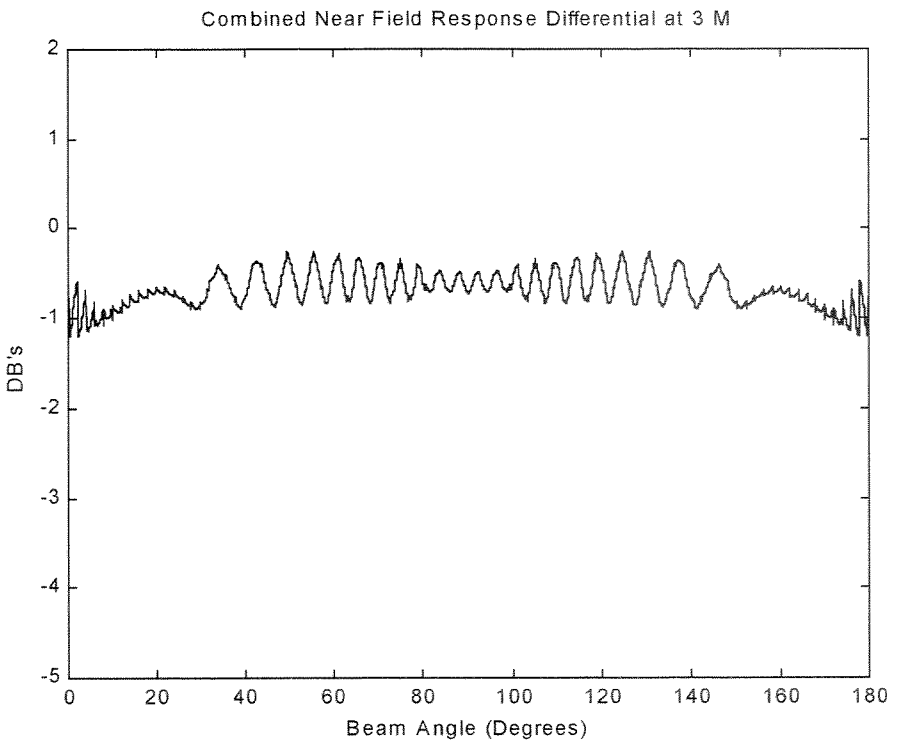

Figure 16. Combined transmit – receive near field effects at 3 m range.

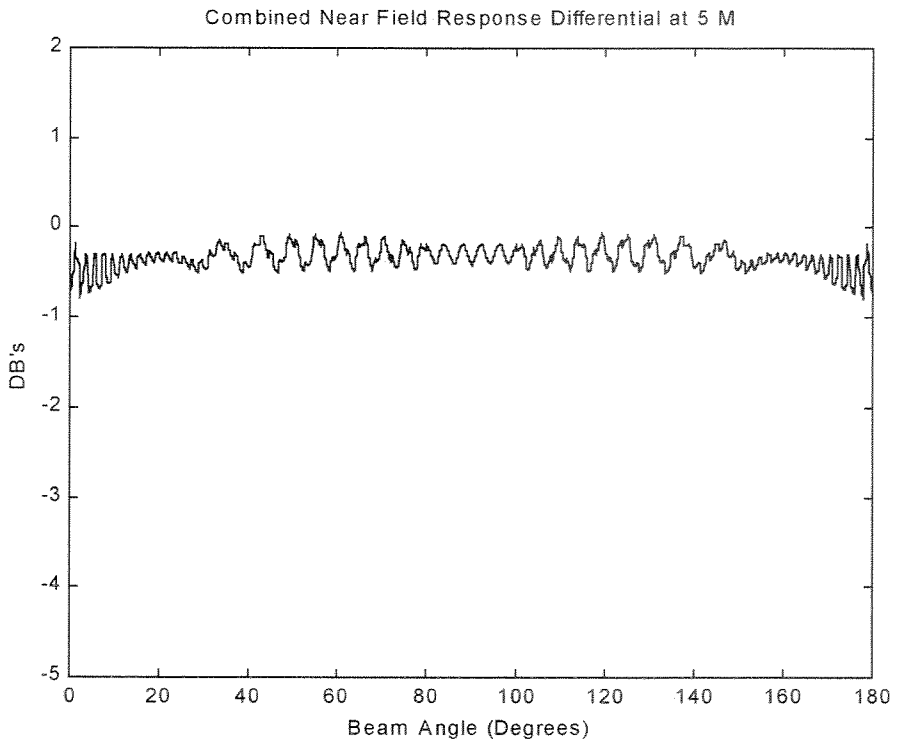

Figure 17. Combined transmit – receive near field effects at 5 m range.

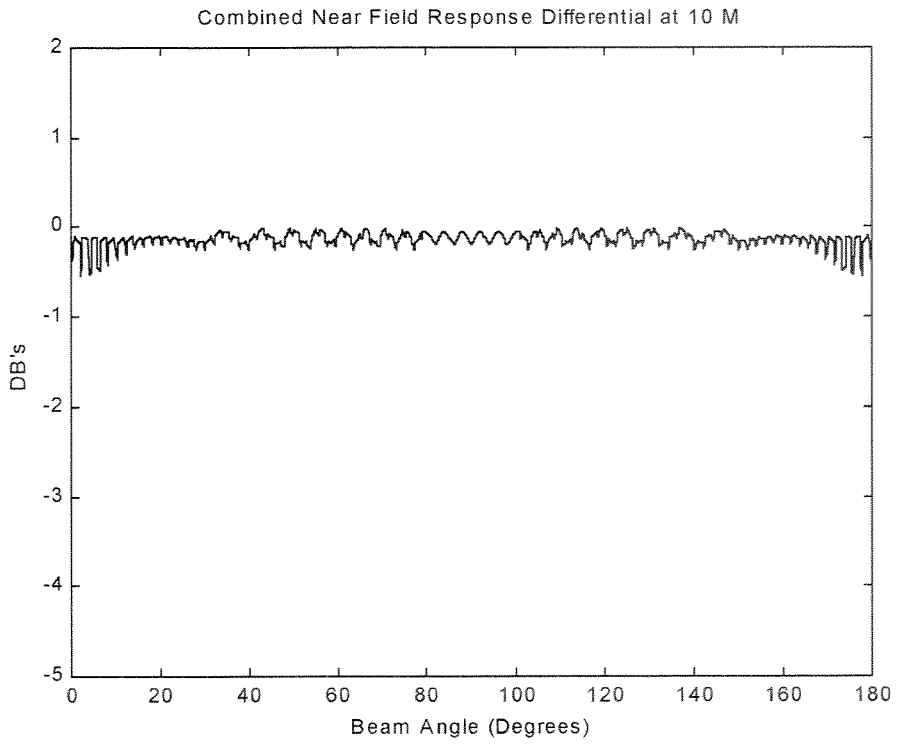

Figure 18. Combined transmit – receive near field effects at 10 m range.

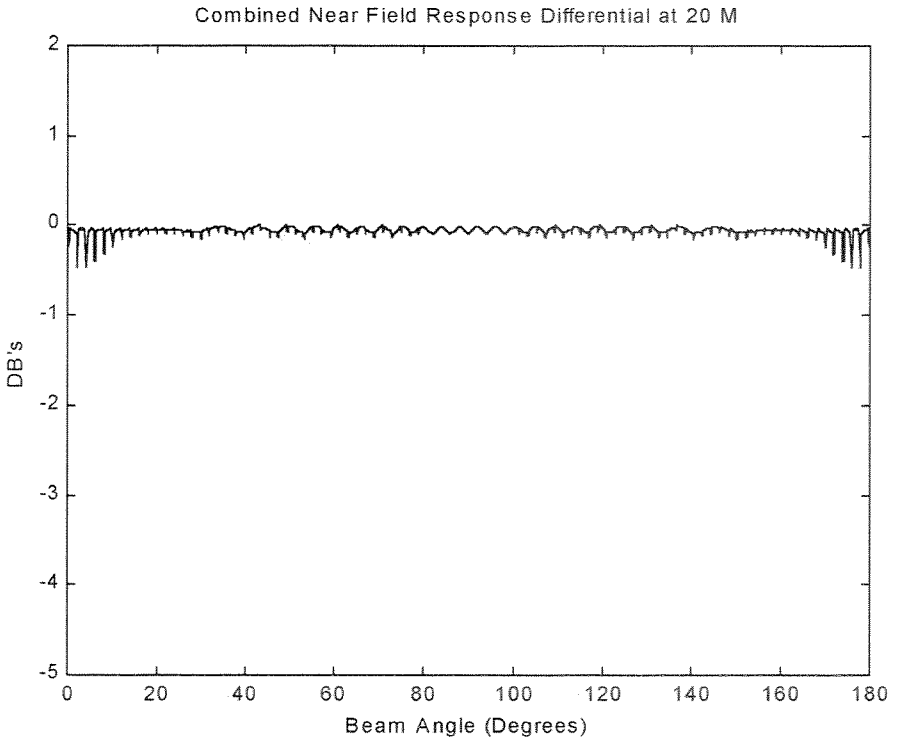

Figure 19. Combined transmit – receive near field effects at 20 m range.

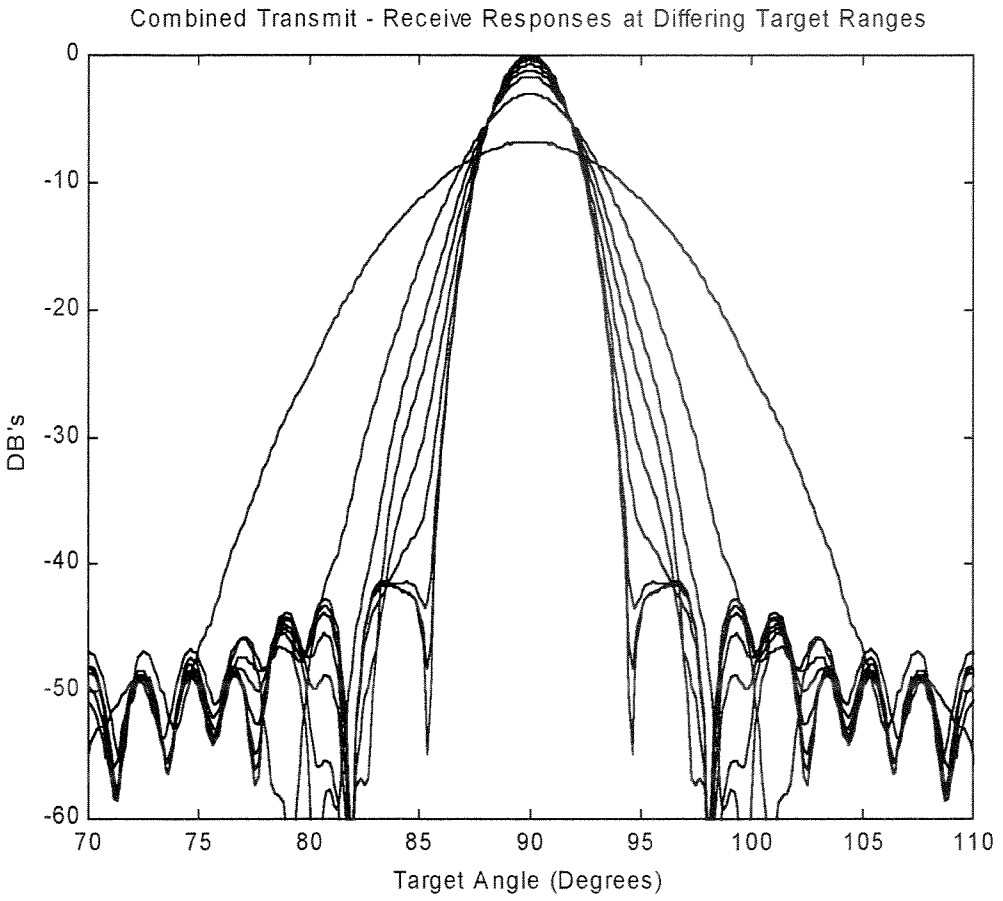

Figure 20. Overlay of combined transmit-receive responses for 90^0 (central) beam and moving target at 1000, 20, 10, 5, 3, 2, 1.5, 1, and 0.5 m ranges.

APPENDIX. BEAMFORMER WINDOW FUNCTION

Both the analytical techniques described and utilized in this report and the SM 2000 real-time processing firmware utilize a window function of the form:

$$W(\theta_b, \theta_n) = a + (1-a)\cos(\pi(\frac{|d - d_m|}{2d_m})) \qquad \text{(A-1)}$$

Windowing is applied to a select fraction of the 155^0 array arc of transducers as projected onto a line normal to the beamforming direction: Let "d" represent the lateral position of a perpendicular dropped from the array transducer at θ_n onto a line drawn normal to the beamforming direction, θ_b. The normal line spans a designated array arc. "Spanning" means that parallels to the beamforming direction drawn from each bounding end of the normal line just enclose a "designated array arc". The "designated array arc" is that arc enclosing all transducers lying within a limiting angle, namely (summation aperture) /2, of the beamforming direction. The summation aperture is arbitrarily set to 150^0 to utilize essentially all of the array elements for the central beams thereby maximizing angular resolution. If an array "end" transducer is encountered within the limiting angle ($150^0/2$), the "end" transducer defines one end of the "designated arc". The bounded normal line is of length $2d_m$ with "d" measured from its mid-point, d_m. The window functional form is always symmetric about the normal line mid-point but not necessarily about the beamforming direction. Asymmetry arises whenever a transducer array "end" is encountered for a specific θ_b, the common case since the 150^0 summation arc length is only slightly less than the 155^0 transducer physical arc length. In this case the effective summation aperture is reduced from its nominal 150^0, and the window function maximum no longer coincides with the beamforming direction.

This report utilizes parameter $a = 0.54$ resulting in a window function of Hamming form, designated "Low Sidelobe" by the manufacturer. The internal firmware offers two additional windowing options with $a = 0.707$ or 0.90 respectively. The latter results in a near-rectangular "boxcar" response offering a higher angular resolution at the expense of theoretically higher sidelobes. The intemediate a value offers a compromise between the Hamming and near-boxcar performances. The use of alternative window functions is amenable to a similar near field analysis to that employed in this report.